

## Quasiperiodic and chaotic behavior due to competition between spatial and temporal modes in long Josephson junctions

L. E. Guerrero and M. Octavio

*Centro de Fisica, Instituto Venezolano de Investigaciones Cientificas, Apartado 21827, Caracas 1020 A, Venezuela  
and Facultad de Ciencias, Universidad Central de Venezuela Apartado 21201, Caracas 1020 A, Venezuela*

(Received 30 September 1987)

We present numerical simulations of long Josephson junctions in the presence of an rf bias and an applied magnetic field, which we model with a sine-Gordon-like equation. We focus our attention on quasiperiodic and chaotic dynamics and their transitions. We show that quasiperiodicity arises from the competition between two incommensurate frequencies: one due to the success of the system in exciting a solitonlike structure and the second one due to the rf drive. We demonstrate the universality of the multifractal structure of the attractor at the onset of chaos.

The transition from quasiperiodicity to chaos has received a great deal of attention in recent years. Quasiperiodic behavior in systems with a small number of degrees of freedom, represented, for example, by ordinary differential equations of first and second order, can be induced if the system is excited by two driving forces with incommensurate frequencies.<sup>1</sup> This is in contrast with certain continuous systems with an infinite number of degrees of freedom that exhibit quasiperiodic behavior in the presence of only one oscillating driving force. This is possible because of the coexistence of the frequency of the driving force and the natural frequency of an oscillating spatial structure. For example, in the case of forced Rayleigh-Bénard convection, the system develops a convective oscillation as a response to the external drive.<sup>2</sup> This competition between space and time may lead to a wide variety of responses of the system, from well-defined periodic motion to a transition from quasiperiodic behavior with two incommensurate frequencies to chaos.

We show for the first time that another high-dimensional system, the long Josephson junctions, as described by a sine-Gordon-like equation, can also exhibit spatiotemporal quasiperiodicity and chaos; this system has previously been studied in the context of chaotic dynamics in long Josephson junctions.<sup>3</sup> In this article a common physical mechanism for the dynamics in space and in time is described: The quasiperiodic behavior is attained via the spontaneous generation of an oscillating and coherent spatiotemporal structure with its own natural frequency that competes with the frequency of the driving force. This is in contrast with numerical simulations<sup>4</sup> in which quasiperiodicity is obtained through the use of an oscillating breather as its initial condition. We also demonstrate, quantitatively, that the transition from quasiperiodicity to chaos in this system is also universal, through the study of the  $f(\alpha)$  spectrum.

The possibility of quasiperiodicity generated via coupling of nonlinear oscillators was proposed by Grotberg and Reiss.<sup>5</sup> We recall that the long Josephson junction can also be viewed as a set of  $n$ -coupled nonlinear oscillators or pendula with  $n \rightarrow \infty$ . In contrast, Josephson junctions with no spatial extent, which are described by the same ordinary differential equation as a driven damped

pendulum, have only been shown to exhibit quasiperiodic behavior in the presence of two driving forces, as studied in analog simulations.<sup>6</sup>

We consider the following model for a long Josephson junction<sup>7</sup> (where long implies length greater than the Josephson penetration depth):

$$\phi_{xx} - \phi_{tt} - \sin\phi = \alpha\phi_t - \rho\sin(\Omega_d t), \quad (1a)$$

$$\phi_x(0, t) = \phi_x(L, t) = \eta. \quad (1b)$$

Here  $\phi$  is the phase difference of the superconducting order parameter between each side of the barrier. In (1), the distance is normalized to the Josephson penetration depth and time is normalized to the inverse of the Josephson plasma frequency. The bias is assumed to be uniform in space with rf amplitude  $\rho$  normalized to the maximum critical current. The term  $\alpha\phi_t$  represents quasiparticle loss. The derivative in time of the phase difference is the voltage across the junction according to the Josephson relation  $\hbar d\phi/d\tau = 2 eV$ , where  $\tau$  is unnormalized time. From integration of this equation it follows that  $\phi$  can be interpreted as a normalized measure of the magnetic flux, that is,

$$\phi = \frac{2e}{\hbar} \int V d\tau = \frac{2\pi}{\Phi_0} \int V d\tau = 2\pi \frac{\Phi}{\Phi_0},$$

where  $\Phi_0$  is the flux quantum. According to this relation, a finite average voltage corresponds to the presence of magnetic-flux quanta. The constant  $\eta$  is a measure of the external magnetic field that induces a surface current in the barrier. In all the results to be presented in this article, parameter values are  $L=5$ ,  $\alpha=0.252$ ,  $\eta=1.25$ , and  $\Omega_d=0.65$ . In what follows we will consider increasing values of  $\rho$  to illustrate the possible observed transitions. We integrated system (1) using a standard implicit finite-difference method dividing the junction into 128 sections. Our integration was started from flat initial conditions  $\phi(x, 0) = 0$  at all points but at the boundaries where we forced the system to satisfy the boundary conditions. In our figures we plot data at the center of the junction.

As will be reported elsewhere,<sup>8</sup> at low values of the rf amplitude ( $\rho < 0.7375$ ), the spatial constraint succeeds in

exciting an oscillating spatial structure that interacts with the driving force, just as in the case of the temperature difference and external forcing in the Rayleigh-Bénard convection. In the case of a long Josephson junction, however, this spatial excitation is coherent and persistent; it is a breather, a solitonic state with an internal degree of freedom, where each of the “coupled pendula” is trapped in this case in one well of its own periodic potential. Thus the junction exhibits no average voltage and therefore zero total magnetic flux has passed by the point  $x$  on the average. In this low-amplitude regime, the temporal response of the oscillating spatial structure locks to the frequency of the driving force, giving either an  $n$ -periodic or a chaotic response at the forcing frequency. In this lower-energy regime, chaotic dynamics are reminiscent of typical low-dimensional systems, particularly of the junction with no spatial extent. At  $\rho \sim 0.7375$  solutions reach the threshold of energy required for the creation of the kinks or fluxons, excitations that propagate along the barrier; this regime is chaotic and amounts in the mechanical analog to the allowance of the pendula in the chain to make complete revolutions. Thus the system exhibits a finite average voltage and therefore magnetic flux quanta can be present. The finite average voltage also supposes that solutions are nontrapped and diffuse from one well to another; it is custom to refer to these solutions as free-running solutions.

With increasing the rf bias, the radiative collisions eventually lead to coalescence of the fluxons into a stable bound state, again just a breather. This collapse of excitations is already known as a fluxon annihilation<sup>9</sup> and can manifest itself in time as a boundary or external crises,<sup>10</sup> i.e., a collision between a chaotic attractor and an unstable periodic orbit that destroys the basin of attraction of the former attractor and gives rise to chaotic transients. The oscillating bound state can oscillate independently of the driving force at the natural frequency ( $\Omega_b = 1.0$ ) of the sine-Gordon equation. In Fig. 1(a) we show the quasiperiodic motion due to a breather state for  $\rho = 2.0$ . Note that in this figure,  $\phi$  covers a range greater than  $2\pi$ , which means that the breather is the result of annihilation of excitations that carried more than a quantum of flux and, therefore, it will no longer be a trapped oscillation in only one well of the periodic potential. The figure can be identified as the major cross section of a torus corresponding to quasiperiodic motion. The origin of quasiperiodic motion can be readily understood by looking at the power spectrum of Fig. 1(b) where we can identify the two peaks of the incommensurate frequencies responsible for the two-torus motion: The peak at  $\Omega/\Omega_d = 1.0$  is due to the rf drive and the one at  $(\Omega/\Omega_d) \approx \sqrt{3}$  is due to the tendency of the spatial structure to give an unlocked answer in terms of the natural frequency of the system, the plasma frequency (equal to 1 in the system of units chosen). Thus the quasiperiodic dynamic results from the competition between the natural response of the system and the drive.

Now we review the salient features of the quasiperiodic dynamics in this system. For increasing rf bias all regions of the torus are not equally visited and we can also note that the initial smoothness of the torus can change to a “wrinkled” look. These two effects are manifestations of

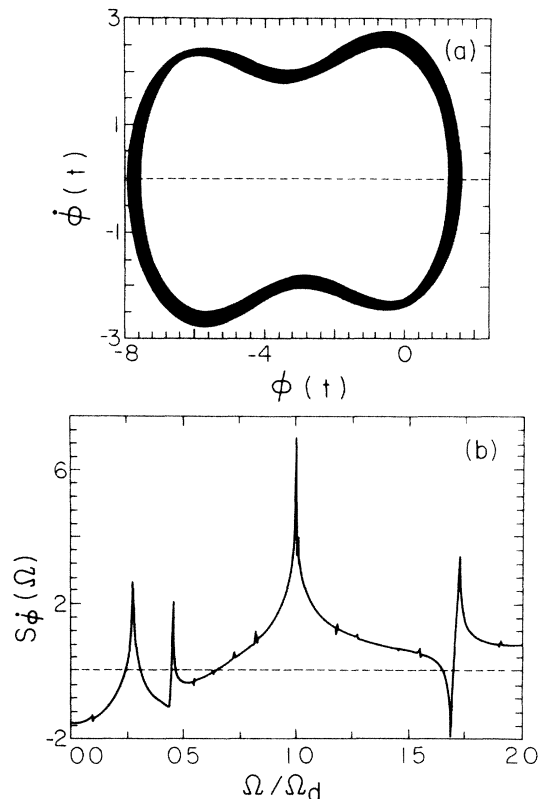


FIG. 1. Quasiperiodic regime. (a) Phase space  $\dot{\phi}_i(t)$  vs  $\phi(t)$  reveals that the quasiperiodicity corresponds to a trapped state in a number of wells of the periodic potential. (b) Voltage ( $V = \dot{\phi}_i$ ) power spectrum  $S_V(\Omega)$  vs  $(\Omega/\Omega_d)$  makes clear the origin of quasiperiodicity: Its higher peaks correspond to the drive and breather frequencies, which are incommensurate.

the competition between the incommensurate frequencies. In the first case, the dominant response is to the frequency of the forcing, because what is occurring is a tendency to lock the response of the system to it and its integer subharmonics. In the second case, it consists of an attempt of the system to create subharmonics of the frequency of the spatial oscillation. Thus the spatial and temporal modes are in competition and the system can present a diversity of responses. The tendency of the system to lock onto the drive eventually results in a periodic motion in  $n$  wells of the periodic potential; on the other hand, the tendency to give a response in terms of the frequency of the uncoupled breather may result in doubling of the torus. The competition between the two incommensurate frequencies via generation of subharmonics eventually leads to a power spectrum with a large number of peaks with characteristic self-similar structure, as shown in Fig. 2(a); this is a critical orbit at the onset of trapped chaos.

The universality of the transition from quasiperiodicity to chaos has been found in a variety of systems.<sup>11</sup> In an experimental situation as well as when dealing with partial differential equations (PDE's), rather than seek universalities at special and not readily discernible points

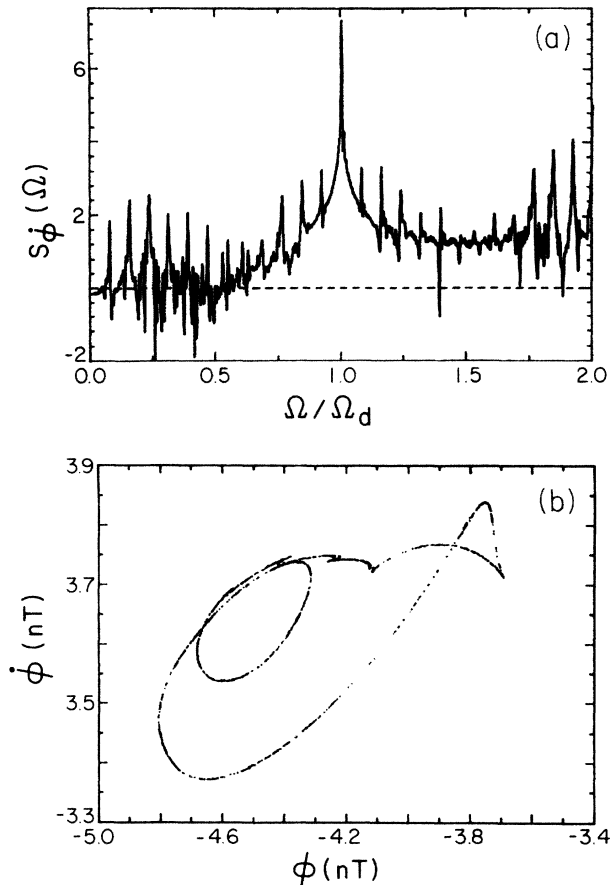


FIG. 2. Critical orbit at the onset of chaos. (a) Voltage ( $V = \phi_i$ ) power spectrum  $S_V(\Omega)$  vs  $(\Omega/\Omega_d)$  evidences that the competition between the two leading frequencies occurs via generation of subharmonics of them. (b) Poincaré map  $\phi_i(T)$  vs  $\phi(T)$  showing the multifractal attractor.

in phase space, what is desirable is to seek more global properties, but still universal, that remain unchanged under smooth changes of coordinates. A complete description of attractors, which are the union of many interwoven fractal sets, can be achieved by characterizing each set with an index  $\alpha$  that describes how the total probability for other points falling in the neighborhood of a given one scales with the size of the region: The function  $f(\alpha)$  is the fractal dimension of the set with index  $\alpha$ .<sup>12</sup> We present in Fig. 3 such a spectrum of scaling indices, or  $f(\alpha)$  spectrum, obtained in the usual fashion<sup>13</sup> for the multifractal attractor at the onset of chaos of Fig. 2(b); the maximum point in the curve exceeds unity because the system is well into the chaotic regime. Comparison with the theory<sup>12</sup>

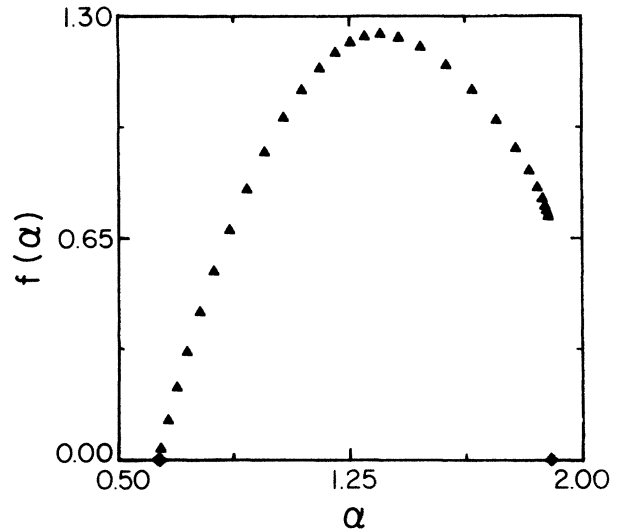


FIG. 3. The  $f(\alpha)$  spectrum calculated for the long Josephson junction exhibits excellent agreement with the theoretical expectation for the external values of  $\alpha$ :  $\alpha_{\min} = 0.6326 \dots$  and  $\alpha_{\max} = 1.8980 \dots$ , also denoted at the abscissa.

and the results obtained with the forced Rayleigh-Bénard system,<sup>13</sup> among others, confirms the universality of the transition.

In addition to this transition to chaos in which the breather profile persists, there is another transition to chaos in this system in which the breakup of the torus is accompanied by a conversion of the spatiotemporal pattern and the breakup of the low-dimensional behavior; at this transition point, the system returns to the higher dimensional free-running chaotic and fluxonic regime. An alternation between free-running chaotic and trapped quasiperiodic regimes has been established, and after each chaotic window, the system generates a breather regime with one additional well. In the fluxonic regime the system is not carried into the total spatiotemporal disorder; rather its dynamics are governed by an attractor because the destruction of fluxons is followed by a new creation of them in an spatiotemporal process analogous to the stretching and folding of a temporal strange attractor. Because the origin of this attractor is the nonlinearity and the dissipation too, we would like to consider this kind of situation as spatiotemporal chaos.

This work has been partially supported by Consejo Nacional de Investigaciones Científicas y Tecnológicas under Project No. S1-1828.

<sup>1</sup>J. P. Sethna and E. D. Siggia, *Physica D* **11**, 193 (1984); C. Grebogi, E. Ott, S. Pelikan, and J. A. Yorke, *ibid.* **13**, 261 (1984).

<sup>2</sup>J. Stavans, F. Heslot, and A. Libchaber, *Phys. Rev. Lett.* **55**, 596 (1985); A. P. Fein, M. S. Heutmacker, and J. P. Gollub, *Phys. Scr. T* **9**, 79 (1985).

<sup>3</sup>J. C. Eilbeck, P. S. Lomdahl, and A. C. Newell, *Phys. Lett.* **87A**, 1 (1981); A. R. Bishop and P. S. Lomdahl, *Physica D* **18**, 54 (1986).

<sup>4</sup>A. R. Bishop, M. G. Forest, D. W. McLaughlin, and E. A. Overman II, *Physica D* **23**, 293 (1986).

<sup>5</sup>J. B. Grotberg and E. L. Reiss, *SIAM Soc. Ind. Appl. Math. J.*

- Appl Math. **45**, 169 (1981).
- <sup>6</sup>D.-R. He, W. J. Yeh, and Y. H. Kao, Phys. Rev. B **30**, 172 (1984); **31**, 1359 (1985).
- <sup>7</sup>A. C. Scott, F. Chu, and S. Reible, J. Appl. Phys. **47**, 3272 (1976).
- <sup>8</sup>L. E. Guerrero and M. Octavio (unpublished).
- <sup>9</sup>A. Barone and G. Paterno, *Physics and Application of the Josephson Effect* (Wiley-Interscience, New York, 1982), p. 284, and references therein.
- <sup>10</sup>C. Grebogi, E. Ott, and J. A. Yorke, Physica D **7**, 181 (1983).
- <sup>11</sup>E. G. Gwinn and R. M. Westervelt, Phys. Rev. Lett. **57**, 1060 (1986), and references therein.
- <sup>12</sup>T. C. Halsey, M. H. Jensen, L. P. Kadanoff, I. Procaccia, and B. I. Shraiman, Phys. Rev. A **33**, 1141 (1986).
- <sup>13</sup>M. H. Jensen, L. P. Kadanoff, A. Libchaber, I. Procaccia, and J. Stavans, Phys. Rev. Lett. **55**, 2798 (1985).